Original Article
J. Korean Wood Sci. Technol. 2025, 53(6): 677-692
https://doi.org/10.5658/WOOD.2025.53.6.677

Journal of the Korean Wood Science and Technology
pISSN: 1017-0715 eISSN: 2233-7180
http://www.woodj.org

Effect of Surface Pre-Treatment on Moisture Dynamics and Drying Defects in Air Drying of Large-Cross-Section Round Timber from Korean Red Pine

Bat-Uchral BATJARGAL[1,2] · Minjee KANG[1,3] · Seong-Hyun LEE[4] · Chang-Jin LEE[5] · Hwanmyeong YEO[1,3,4,†]

ABSTRACT

Large-cross-section timber is susceptible to defects such as surface checking and blue staining during the protraction process. Uncontrolled air drying without pre-treatment of these materials often leads to these defects and negatively impacts product quality and manufacturing costs. To address these issues, this study implemented real-time monitoring of temperature and moisture changes within the internal and external environments of the timber during drying. This research was conducted using Korean red pine (*Pinus densiflora*) round timber with a diameter of 45 cm under air-drying conditions. Untreated specimens were compared with those subjected to various surface pre-treatments (end sealing, end coating, and lateral coating). Changes in the amount of water released from timber were monitored using a load cell, while environmental and internal wood conditions were measured and recorded in real-time using a data logger with temperature and humidity sensors. The findings revealed that immediate air drying following debarking successfully mitigated blue staining, but it was consistently associated with the development of checks. Surface pre-treatments slowed the drying rate and consequently suppressed the occurrence of checking; however, defects were not entirely prevented. This study emphasizes the necessity of effective heat and moisture transfer control through appropriate physical quantity detection during large timber drying. These findings are expected to contribute to the optimization of drying processes and development of real-time monitoring technologies for industrial applications.

Keywords: red pine, large-cross-section timber, air drying, pre-treatment, moisture content, drying defects, monitoring

1. INTRODUCTION

Korean red pine has been used extensively in various sectors, including architecture, civil engineering, furniture, packaging, and pulp production (Han *et al.,* 2019a; Kim *et al.,* 2020; Lee *et al.,* 2022; Park *et al.,* 2024; Shin *et al.,* 2025). Specifically, large-cross-section timber is critical for the preservation and restoration of wooden cultural heritage sites, such as royal palaces and temples, where it is used in columns and beams (Jiang *et*

Date Received October 22, 2025; Date Revised October 27, 2025; Date Accepted November 3, 2025; Published November 25, 2025
[1] Department of Agriculture, Forestry and Bioresources, Seoul National University, Seoul 08826, Korea
[2] Training and Research Institute of Forestry and Wood Industry, Mongolian University of Science and Technology, Ulaanbaatar 14191, Mongolia
[3] Research Institute of Agriculture and Life Sciences, Seoul National University, Seoul 08826, Korea
[4] Department of Forest Sciences, Seoul National University, Seoul 08826, Korea
[5] Department of Wood Science and Technology, Jeonbuk National University, Jeonju 54896, Korea
[†] Corresponding author: Hwanmyeong YEO (e-mail: hyeo@snu.ac.kr, https://orcid.org/0000-0002-1779-069X)
© Copyright 2025 The Korean Society of Wood Science & Technology. This is an Open-Access article distributed under the terms of the Creative Commons Attribution Non-Commercial License (http://creativecommons.org/licenses/by-nc/4.0/) which permits unrestricted non-commercial use, distribution, and reproduction in any medium, provided the original work is properly cited.

al., 2023; Lee, 2020; Park *et al.,* 2020; Srisuchart *et al.,* 2023). Air drying is a simple, common, and financially nonintensive method for reducing the moisture content (MC) of large timber (Erber *et al.,* 2017; Lee *et al.,* 2024; Routa *et al.,* 2015). However, it is influenced by multiple factors, including the initial MC, environmental conditions, wood species, and drying strategy, often resulting in prolonged drying times and potential defects that degrade wood quality (Kim *et al.,* 2023). Therefore, the effective management of key parameters during the drying process is essential for timber to reach the target MC while maintaining structural integrity and performance.

Despite its cost-effectiveness, the air drying of large-cross-section timber presents significant challenges, primarily owing to the difficulty in achieving precise MC control (Ogueke *et al*., 2015). Uncontrolled, slow air drying often leads to steep moisture gradients, resulting in various drying defects such as deep surface checking and warping, which severely impact product quality and manufacturing costs (Thybring and Fredriksson, 2021). Furthermore, the final MC of timber in air-drying systems can vary significantly depending on seasonal and climatic conditions, rendering the planning of industrial drying schedules highly complex (Han *et al*., 2019b). Therefore, developing cost-effective and practical surface pre-treatment strategies is essential to mitigate these defects and enhance the predictability and quality of air-dried large timber, ultimately improving its long-term durability (Sehlstedt-Persson and Wamming, 2010).

Environmental factors, including temperature, relative humidity (RH), and air circulation, play a significant role in air drying (Ugwu *et al.,* 2021). Higher temperatures increase the moisture-holding capacity of air, and a strong airflow enhances surface moisture removal. However, excessively fast evaporation can rapidly dry the wood surface, leading to drying stress and defects such as surface and internal checking (Avramidis *et al*., 2023; Batjargal *et al*., 2023; Bond and Espinoza, 2016).

These findings emphasize that meticulous control during the drying process is vital for improving final timber quality. Physical pre-treatments, such as high-temperature steaming or kerfing before drying, can relieve internal growth stress and alter moisture flow paths, thereby preventing internal checking and enhancing dimensional stability.

The initial MC significantly affects both drying time and final MC (Möttönen, 2006). Consequently, real-time monitoring of the wood MC and environmental conditions is necessary during drying (Elustondo *et al.,* 2023; Lazarescu *et al.,* 2010; Schmidt and Riggio, 2019). Studies by Kang *et al.* (2011, 2016) indicated that monitoring the strain distribution during the initial drying stage helps to mitigate the potential for defect occurrence. The interaction between wood and moisture is central to wood processing and utilization (Thybring and Fredriksson, 2021), because moisture directly influences the physical and mechanical properties, durability, and dimensional stability of wood. Specifically, the anisotropy of shrinkage and uneven moisture gradient that develops during drying are the main sources of drying stress, which causes warping and cracking (Dietsch *et al*., 2015; Fu *et al.,* 2015, 2023; Zinad and Csilla, 2024).

Considering this problem, the present study aims to develop a drying control technique for the efficient drying of large-cross-section timber without defects, including surface checking and blue staining, and to identify the factors influencing the drying rate and defect initiation. The findings from the study are expected to contribute to the optimization of the drying process, prediction of drying time, and enhancement of the final product quality.

2. MATERIALS and METHODS

2.1. Test specimens and drying procedure

Debarked red pine (*Pinus densiflora*) round timber

with a diameter of 450 mm and total length of 3,000 mm was used for this investigation. Four round timber specimens, each 600 mm long, were obtained from the primary processed round timber (Fig. 1). For material characterization, 20 mm-thick disk-shaped samples were collected from each end of the specimens to determine the initial MC and basic wood density (WD). Disks for MC were further subdivided into 77 smaller pieces to conduct an in-depth analysis of the initial MC distribution across the locations. Before sectioning the logs, the average basic WD was determined to be 0.42 g/cm^3, and the average initial MC was 93%.

The drying experiment was conducted in an air-drying yard. The specimens were housed in a simple tent structure to prevent rain ingress [Fig. 2(a)]; however, the sides remained open to allow for natural airflow and ventilation, typical of outdoor air-drying conditions. The target final MC was set at 24%, a threshold based on the requirements of the 2024 National Heritage Repair Standard Specification that large-cross-section timber used for cultural heritage restoration must have an MC of 24% or less (National Heritage Administration, 2024). This standard is crucial because maintaining timber below 25% MC helps prevent or minimize discoloration, decay, and mold, thereby reducing the risk of long-term deterioration. This target level is consistent with the established standards for timber dimensions and aligns with the MC goal in large-cross-section timber drying research (Batjargal *et al.,* 2025; Han *et al.,* 2019a).

We compared four drying conditions, an untreated control (C) and the following three surface pre-treatment applications designed to mitigate surface checking (Fig.

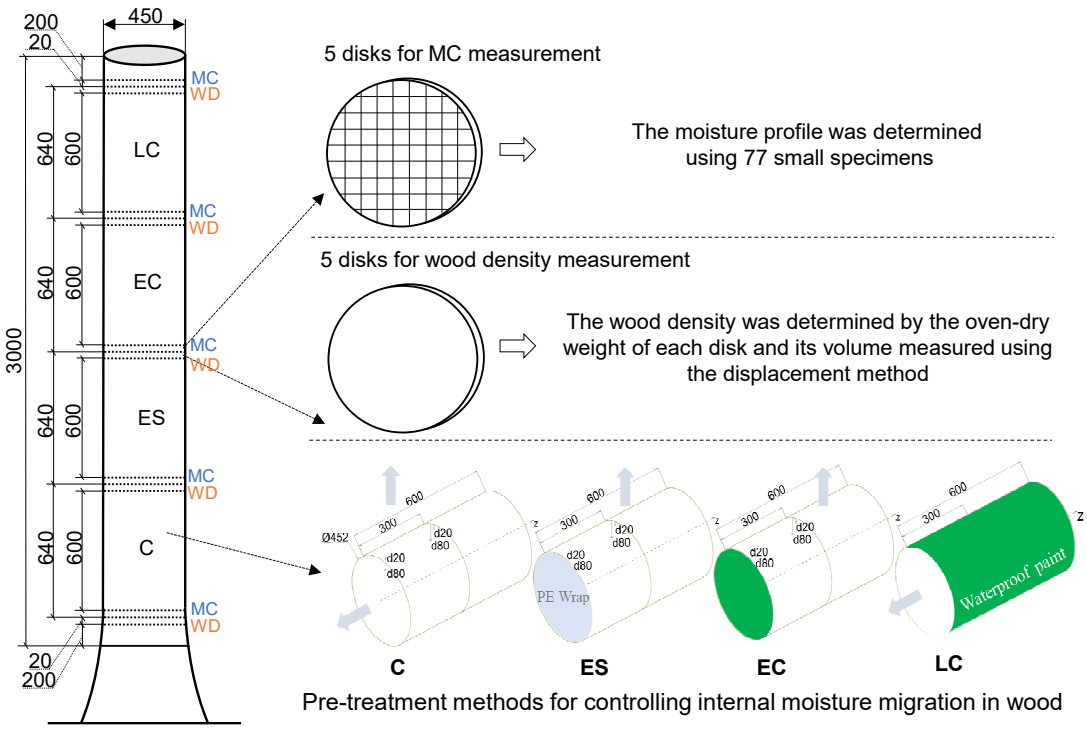

Fig. 1. Illustration of the experimental procedure. MC: moisture content, C: control, ES: end sealing; EC: end coating; LC: lateral coating.

Fig. 2. Wood specimens mounted in a case with a load cell (a); VAISALA HMP60 humidity and temperature sensor (b); TLC-1t tension load cell (c); and iButton humidity and temperature sensor (d) and K-type thermocouples (e), inserted at multiple positions to measure the moisture and temperature gradient between the surface and core of the wood specimen.

1): end sealing (ES) using polyethylene sheets on the cross-sectional ends, end coating (EC), and lateral coating (LC) using a waterproof urethane paint (New Watertan, Samhwa Paints Industrial. Co, Seoul, Korea). The duration of air-drying for all the specimens was approximately 515 days (from January 2024 to June 2025).

2.2. Monitoring of drying conditions

Real-time monitoring was performed to track changes in the MC and environmental parameters during drying.

2.2.1. Wood weight and environmental monitoring

A tension load cell [TLC-1t, Bongshin, Osan, Korea; Fig. 2(c)] was used to measure the weight of the specimens at 6 h intervals [Fig. 2(a)]. A CR1000X data logger was used to record external environmental factors (ambient temperature, RH, and wind speed) and internal wood temperature at 30 s intervals [Fig. 2(e)]. Additionally, temperature and RH at various internal wood locations were recorded every hour using DS1923 Hygrochron iButton sensors (temperature range: −20 to +85℃, accuracy ±0.5℃; RH range: 0% to 100%). These measurements enabled real-time monitoring of the localized MC during the drying process [Fig. 2(d)].

2.2.2. Wood density calculation

The volume [$V_{(disk)}$] of the 20 mm-thick disk specimens was measured using the water displacement method [Fig. 3(a)], and the oven-dry weight ($W_{od(disk)}$) was determined by the oven-dry method. The basic WD [$\rho_{(disk)}$] was then calculated using Equation (1):

$$\rho_{(disk)} = \frac{W_{od(disk)}}{V_{(disk)}}, \quad (1)$$

Where $\rho_{(disk)}$ is the basic WD of the disk specimen (kg/m^3), $W_{od(disk)}$ is the oven-dry weight of the disk

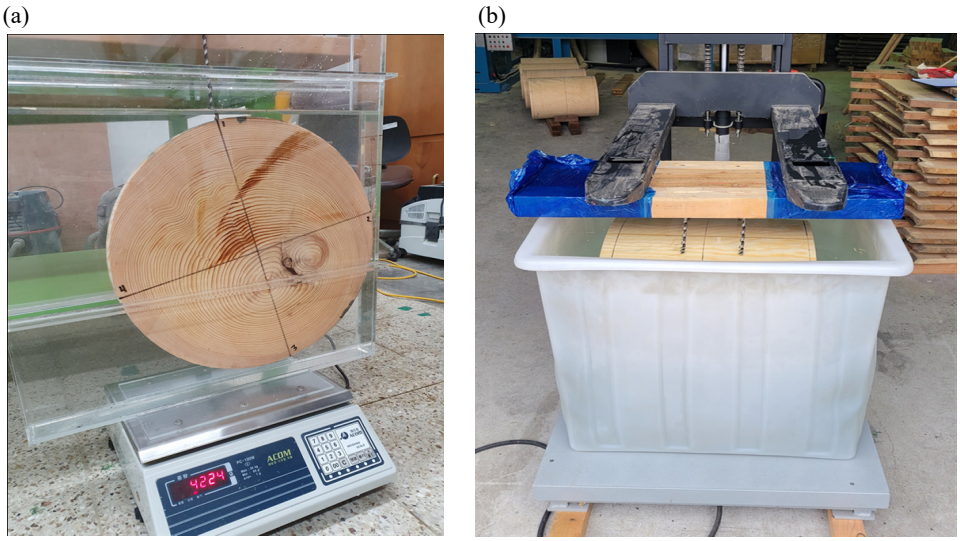

Fig. 3. Volume determination of specimens using the water displacement method. (a) 20 mm-thick disk-shaped sample; (b) 600 mm-long test specimen.

specimen (kg), and $V_{(disk)}$ is the volume of the disk specimen (m^3).

2.2.3. Measurement of initial moisture content of wood

The volume [$V_{(timber)}$] of the 600 mm-long test timber specimen was measured using the water displacement method [Fig. 3(b)]. The estimated oven-dry weight of the timber specimen [$W_{od(timber)}$] was calculated using the specimen volume [$V_{(timber)}$] and average basic WD [$\rho_{(disk)}$] of the disk samples, as shown in Equation (2):

$$W_{od(timber)} = V_{(timber)} \times \rho_{(disk)} \quad (2)$$

The MC of the specimen [$MC_{(timber)}$] over time was evaluated using the weight of the moist specimen [$W_{g(timber)}$] measured by the load cell and the estimated oven-dry weight [$W_{od(timber)}$], according to Equation (3):

$$MC_{(timber)} = \frac{W_{g(timber)} - W_{od(timber)}}{W_{od(timber)}} \times 100\%, \quad (3)$$

Where $MC_{(timber)}$ is the MC of the 600 mm specimen, $W_{od(timber)}$ is the estimated oven-dry weight of the specimen (kg), and $W_{g(timber)}$ is the green moist weight of the specimen (kg).

2.2.4. Internal temperature and moisture content estimation

Sensors were installed in both the shell and core layers to monitor the internal temperature and humidity changes. Four K-type thermocouples were inserted at depths of 20 mm and 80 mm from the lateral surface to record the internal wood temperature at 30 s intervals [Fig. 2(e)]. A compact humidity sensor iButton (Hygrochron DS1923, Maxim Integrated, San Jose, CA, USA) was inserted at a depth of 80 mm to monitor the temperature and humidity changes at 1 h intervals [Fig. 2(d)].

The recorded temperature and humidity data were used to estimate the equilibrium moisture content (EMC) at different locations within the specimen by applying the Hailwood–Horrobin equation, and the trend of localized changes in EMC during drying was analyzed.

The Hailwood–Horrobin EMC equation is represented in Equation (4):

$$EMC = \frac{RH}{A + B \cdot RH - C \cdot RH^2}$$

$$A = \frac{W}{0.018} \cdot \left[\frac{1}{K_2 \cdot (K_1 + 1)}\right]$$

$$B = \frac{W}{1.8} \cdot \left[\frac{K_1 - 1}{K_1 + 1}\right]$$

$$C = \frac{W \cdot K_1 \cdot K_2}{180 \cdot (K_1 + 1)}$$

$$W = 0.2234 + 0.0007 \cdot T + 0.000019 \cdot T^2$$

$$K_1 = 4.73 + 0.048 \cdot T - 0.0005 \cdot T^2$$

$$K_2 = 0.706 + 0.0017 \cdot T - 0.000006 \cdot T^2, \quad (4)$$

Where EMC is the equilibrium moisture content (%); RH is the internal relative humidity (%); and W, K_1, and K_2 are the coefficients of the sorption model developed by Hailwood–Horrobin (Ra, 2014; Simpson, 1973).

3. RESULTS and DISCUSSION

3.1. Initial moisture content and wood density

MC and basic density of specimens taken from various longitudinal positions [at 0.22 m (one side edge), 0.86 m, 1.50 m, 2.14 m, and 2.78 m (the other side edge) from the butt end] of the round timber were measured. The initial MC of the disks cut from both sides of the wood was low, whereas that in the central part was high. In contrast, the basic WD was uniform along its length (Fig. 4).

This pattern differs somewhat from previous studies that measured moisture distribution within freshly felled logs (Kollmann and Côté, 1968; Simpson, 1991). In these studies, MC initially increased gradually toward the top of the log, while basic density showed the opposite trend owing to differences in wood formation along the tree length. A higher initial MC in the log-top was associated with a greater proportion of juvenile wood, which has larger cell lumens and thinner cell walls. Conversely, the butt end showed a higher density, characterized by a higher proportion of mature wood with thicker cell walls and higher lignin content.

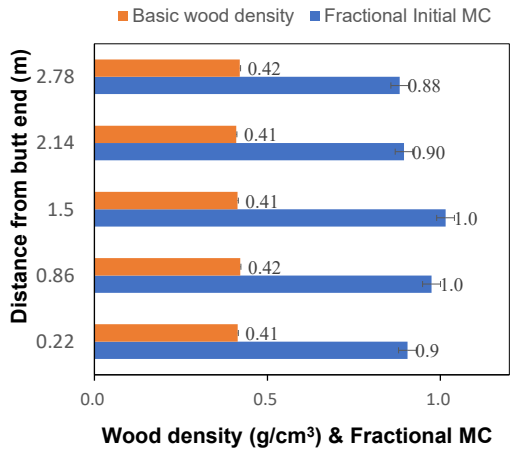

Fig. 4. Basic wood density and fractional initial moisture content of timber.

However, the raw timber prepared in this study was stored with the ends exposed after logging, resulting in both ends drying. The results of this study showed that the variation in longitudinal WD was smaller than that in the MC.

The error between the initial MC calculated on the basis of the basic WD [Equation (1)] and the initial MC calculated using the oven-drying method was within 1.7%, demonstrating the high validity of the MC determination method based on the basic WD.

3.2. Initial moisture content distribution profile

The MC of sapwood exceeded 100%, whereas that of heartwood was approximately 30%. This significant difference indicates that the shell layer generally contains

substantially more moisture than the core layer (Fig. 5), which is consistent with previous observations (Batjargal *et al.,* 2023, 2025).

3.3. Average change in moisture content

Distinct differences in drying rates were observed among the specimens (Fig. 6). Although the sample size was limited to one specimen per treatment owing to the large cross section, the observed deviation in drying kinetics and defect occurrence were analyzed to ensure the reliability of the comparative results.

The average MC of all specimens dropped sharply to below 50% during the initial 180 days. C exhibited the fastest drying rate, suggesting a close relationship between the drying rate and the occurrence of drying defects [Fig. 6(a)]. The control specimen exhibited the largest temporal variation in the onset of surface checking compared with the treated groups.

Despite the use of urethane waterproof paint, the EC treatment failed to completely restrict moisture loss from the cross-sections. Discoloration and mold growth were observed in the cross-sections of the ES specimens. This undesirable outcome is likely attributable to the continuation of wet condition in cross-section areas during the prolonged air-drying period, which fosters an environment conducive to fungal development.

For the LC specimens, the surface application inhibited moisture evaporation from the high-MC surface layer, thereby reducing the initial drying rate. This

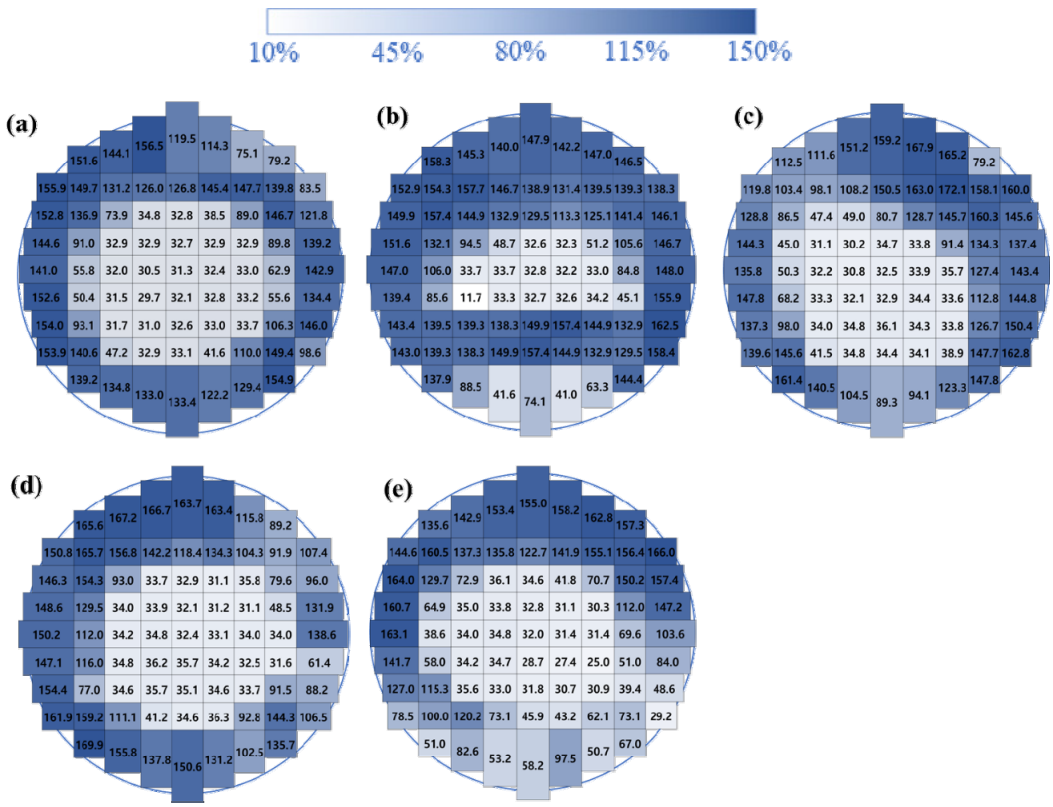

Fig. 5. Initial MC profiles in wood disk at intervals of (a) 220 mm, (b) 860 mm, (c) 1,500 mm, (d) 2,140 mm, and (e) 2,780 mm from the log butt. MC: moisture content.

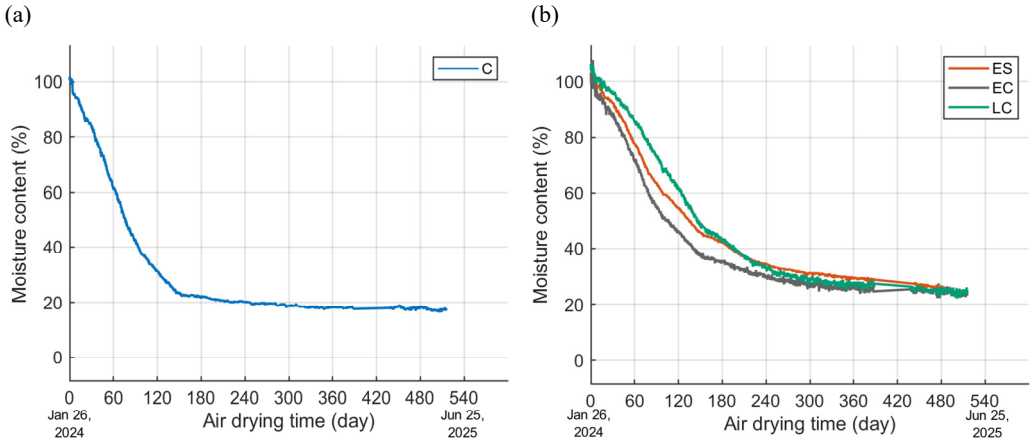

Fig. 6. Drying behaviors of large-cross-section timber. (a) Control; (b) surface pre-treatments. C: control, ES: end sealing, EC: end coating, LC: lateral coating.

drying delay effectively delayed and suppressed checking by inhibiting the rapid surface shrinkage caused by quick drying. Notably, the LC specimen showed the least variation in defect formation, highlighting the uniform effectiveness of this treatment for surface control.

However, visual monitoring revealed that the splits continued to form after approximately 180 days. While the LC treatment significantly slowed the drying process during the initial stage, the average MC of the LC specimens gradually converged with that of the other groups after approximately 300 days. At the conclusion of the study after 515 days, the final MC values were recorded as follows: C: 17.5%, ES: 24.7%, EC: 23.5%, and LC: 25.2%. The experiment was terminated at 515 days to compare the long-term performance of the treatments over a fixed duration.

Despite the superior defect mitigation achieved by the LC treatment, the application of such treatments to full-sized timber (longer than 60 cm) may present practical challenges for industrial application, and the resulting drying characteristics could vary depending on the scale and method of application.

The drying rates of the four treated specimens, including C, were compared by dividing the total drying period into five intervals (Table 1).

During the initial drying period, specifically from 0 to 200 days, a clear difference in the drying rates was observed among the treated specimens. The specimens dried in the following order of decreasing speed: C > EC > ES > LC. This trend is consistent with the general principle that specimens with larger exposed surface areas that are in contact with ambient air dry more rapidly. This result was confirmed by the LC specimens, which exhibited the most effective barrier against moisture loss from the main lateral surface and showed the lowest initial drying rate.

Table 1. Comparison of MC reduction (%) for treated and untreated specimens over time

Day	C (%)	ES (%)	EC (%)	LC (%)
0–100	63.3	43.6	49.7	37.6
100–200	16.5	20.9	18.7	29.5
200–300	1.9	7.5	6.4	10.3
300–400	1.2	2.3	1.8	1.5
400–500	0.2	4.5	1.1	2.6

MC: moisture content, C: control, ES: end sealing, EC: end coating, LC: lateral coating.

Furthermore, the results suggest that the moisture barrier effects of the ES and LC are greater than those of the EC. The EC-treated specimens generally exhibited a faster drying rate than the ES and LC specimens, indicating that the full coverage provided by the LC treatment was the most effective method for restricting initial moisture loss.

As the drying period was extended, the drying rate decreased sharply. From 300 to 500 days, all four treated specimens showed similar and very low drying rates.

This decrease indicated that the MC of the specimens approached the EMC determined by the surrounding atmospheric conditions. This final stage is characterized by a stable and slow moisture loss as the wood gradually equilibrates with the ambient air, regardless of the initial surface treatment method.

3.4. Climatic conditions

Climatic conditions, including seasonal temperature and RH changes, were recorded (Fig. 7). During the air-drying period, the maximum temperature was 38.0℃, the minimum was −13.1℃, and the average was 12.9℃. Air humidity exhibited the largest diurnal variation, ranging from 19% to 99% with an average of 64.4% [Fig. 7(b)]. The substantial diurnal and seasonal fluctuations in temperature and RH contributed to the high variability observed in the overall drying kinetics, with the untreated (C) specimen being most susceptible to these climatic extremes.

A tendency for the MC to decrease was noted during winter and early spring (February to May) when the EMC was lower, corresponding to a low RH [Fig. 7(a)]. This trend was reflected in the application of the Hailwood−Horrobin equation, where a lower RH resulted in a lower calculated EMC. The drying rate decreased during the winter months despite the decrease in RH, which was likely due to low temperatures.

3.5. Internal temperature of wood and humidity dynamics

Fig. 8 presents the internal temperature of the wood. These data illustrate the internal temperature dynamics during drying, measured by sensors embedded at strategic locations: depths of 20 mm and 80 mm from the surface and 50 mm and 300 mm from the end face of the timber. A subtle temperature difference was obser-

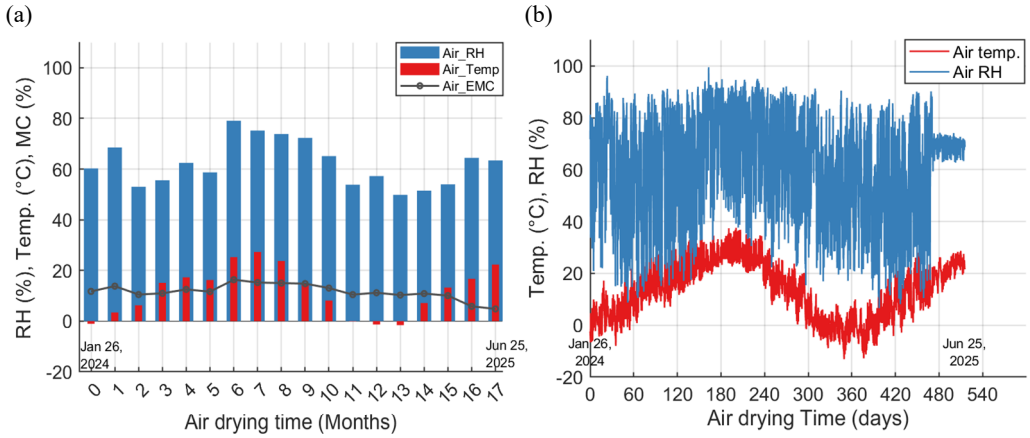

Fig. 7. Weather data recorded during air drying. (a) Monthly average of outdoor air conditions; (b) Results measured at 30 s intervals. RH: relative humidity, MC: moisture content, EMC: equilibrium moisture content.

ved, depending on the specific longitudinal position and depth within the wood (Fig. 8).

Internal temperature and humidity were measured using compact humidity sensors (iButton sensor; DS1923 Hygrochron) installed at a depth of 80 mm in the middle section of the specimens. The recorded data were used to estimate the localized MC (Fig. 9). A significant challenge arose during the initial drying phase (the first 210 days) because of frequent sensor malfunction attributed to the extremely high initial MC of wood. To ensure the reliability of the localized internal data, the sensors were reinstalled after the initial 210-day period. This reinstallation was strategically performed at a point where the internal RH dropped below 90%, indicating that the MC was sufficiently reduced to allow the sensors to operate normally, excluding the electrical interference caused by liquid moisture (free water). Consequently, the sensor data for the first 210 days were considered unreliable and unavailable. To compensate for this data gap, an estimated trend line for internal temperature,

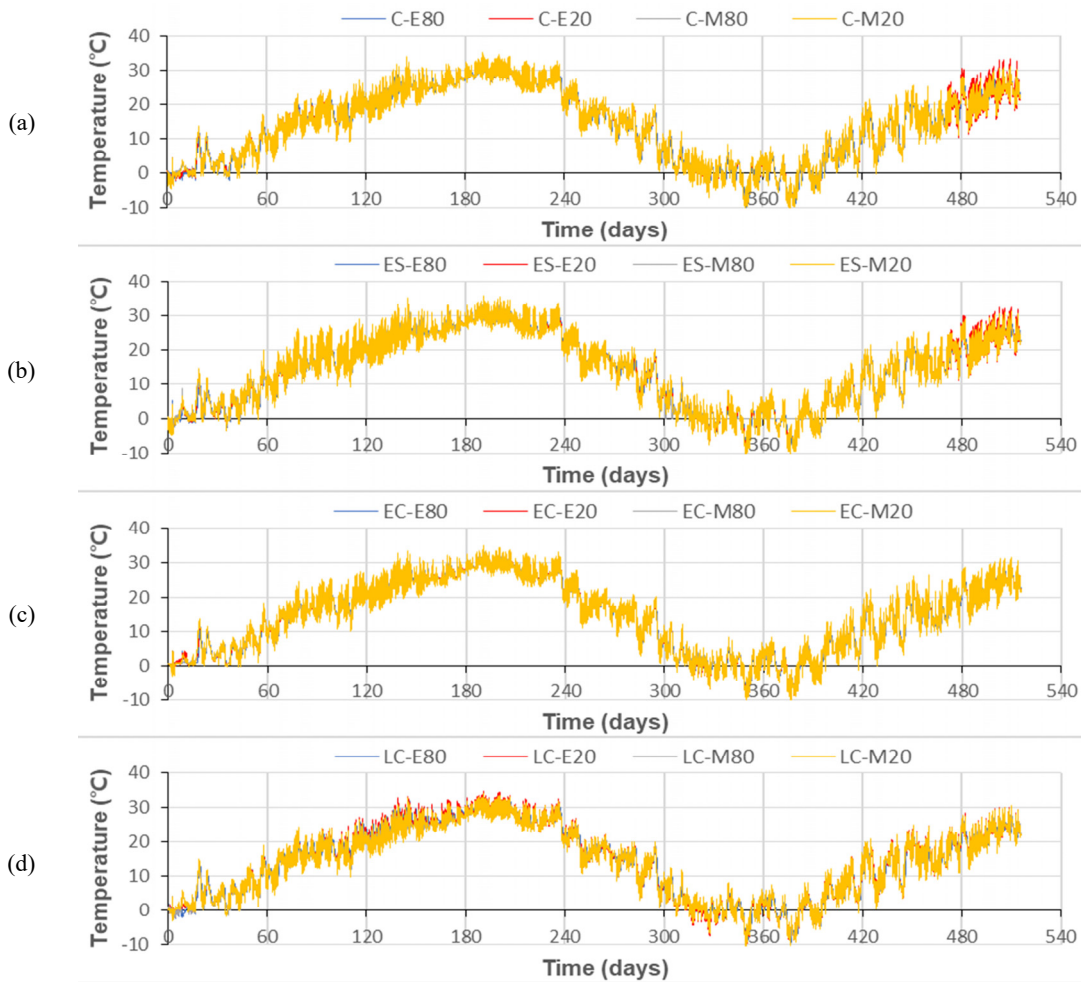

Fig. 8. Internal wood temperature for (a) control (C); (b) end sealing (ES); (c) end coating (EC); (d) lateral coating (LC).

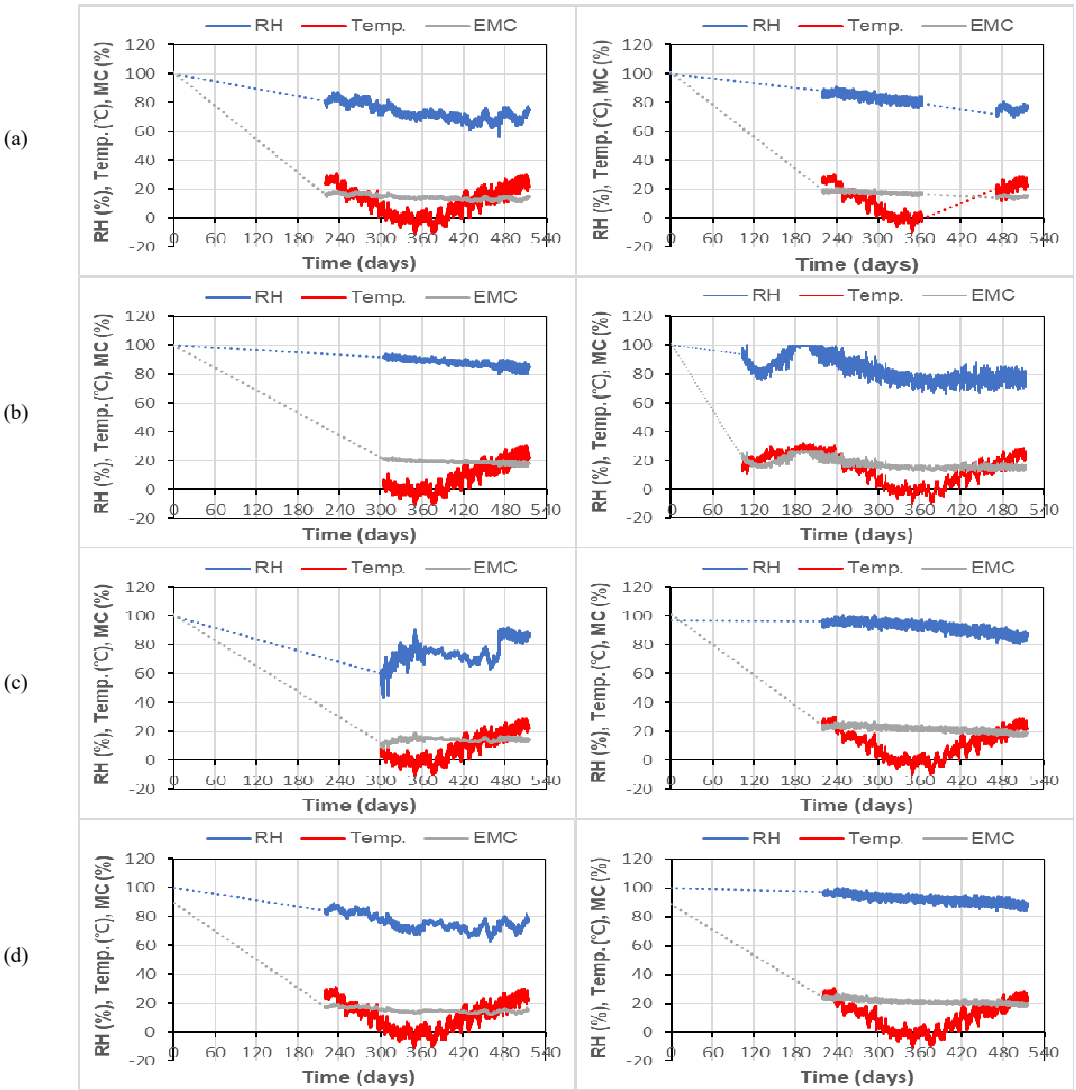

Fig. 9. Temperature and MC estimated from measurements with temperature and humidity sensors. (a) Control; (b) end sealing; (c) end coating; (d) lateral coating. RH: relative humidity, MC: moisture content, EMC: equilibrium moisture content.

humidity, and MC was established by extrapolating the initial MC and using empirical data collected from the air-drying yard.

The RH and EMC relationship can be utilized to adjust wood drying schedules, with the dry-bulb temperature and RH of the ambient air being critical factors in determining the EMC conditions. In a given environment, the MC of wood is driven by the RH and converges toward the EMC value over time (Mori *et al.,* 2025).

To enhance the interpretability of these experimental results, the integration of numerical modeling is suggested, which would lead to more compelling conclusions.

3.6. Drying characteristics and defect occurrence

Drying defects in timber are primarily attributed to drying stress. When the influence of inherent growth stress is excluded, the stress arises mainly from shrinkage anisotropy and a steep MC gradient. These two factors are the primary causes of wood deformation and cracking (Fu *et al.*, 2023).

To provide a quantitative assessment of the drying defects, surface checks were performed and recorded after the 515-day drying period. The severity of the checks was quantified by measuring the maximum crack width and the total cumulative crack area on the cylindrical surface of each large-cross-section specimen. For this assessment, only surface checks with widths exceeding 1 mm were considered, as smaller checks are typically removed during post-drying processes. All specimens were analyzed using digital Vernier calipers (Multicomp PRO MP012475, Mitutoyo, Kawasaki, Japan). The results (Fig. 10; Table 2) confirm the visible differences in the defect severity among the treatments.

Specimen C exhibited the most severe defects, with a average crack width of 5.29 mm and a total crack area of 66.99 cm^2. These defects were characterized by deep, extensive radial checks across the surface, confirming the high susceptibility of large-diameter timber to rapid, uncontrolled drying. The rapid and early surface moisture loss in Group C led to severe case hardening, resulting in significant internal stress that quickly ex-

Fig. 10. Drying defects of large-cross-section timber. (a) Control; (b) end sealing; (c) end coating; (d) lateral coating.

Table 2. Quantitative assessment of surface checks for each pre-treated specimen after 515 days of air drying

Treatment	Average check width (mm)	Average check length (mm)	Number of surface checks	Total area of surface checks (cm^2)	Primary defect type
C	5.29	316.61	3	66.99	Splits, surface checks, end checks
ES	2.25	292.92	11	72.49	Split, surface checks, biological deterioration at the cross section
EC	3.75	268.38	5	50.26	Split, surface checks
LC	1.98	316.44	5	31.32	Suppressed surface checks, end checks

C: control, ES: end sealing, EC: end coating, LC: lateral coating.

ceeded the tensile strength of the timber.

The ES and EC treatments showed moderate improvement compared with the control, indicating that end-grain moisture loss control alone was insufficient to prevent significant surface defects in large timber. The ES specimen had a average crack width of 2.25 mm and a total crack area of 72.49 cm^2, whereas the EC specimen showed a average width of 3.75 mm and an area of 50.26 cm^2. Notably, the ES and EC groups experienced the large overall total crack areas, suggesting that restricting only the end-grain diffusion forces moisture loss through the lateral surface, possibly exacerbating the surface stress and defects in the cylinder face compared with that in the uncontrolled C specimen.

The LC treatment proved to be the most effective method for defect mitigation. The LC specimen had a average crack width of only 1.98 mm and a total crack area of 31.32 cm^2. The observed defects were primarily minor, isolated hairline checks that formed late in the drying process (after approximately 180 days) when the internal moisture gradient became pronounced. This result quantitatively supports the visual observation (Fig. 10) that surface modification significantly suppresses the rapid surface checking caused by the differential shrinkage between the surface and core layers, thereby improving the overall quality of the dried timber. The success of the LC is directly attributable to its ability to slow the initial drying rate of the shell, effectively mitigating the formation of a severe MC gradient and delaying the onset of critical drying stresses.

While the current study successfully quantified the final defects through visual observation and measurement, continuous research focusing on the measurement or estimation of internal drying stress within timber is essential to fundamentally understand the mechanisms of defect formation and to further enhance defect suppression strategies.

We only considered surface checks larger than 1 mm in the digital Vernier caliper (Multicomp PRO MP012475; Table 2). Surface checks wider than 1 mm were measured because, during the post-drying process, smaller checks (less than 1 mm) are typically eliminated through processes such as planing.

4. CONCLUSIONS

In this study, various surface pre-treatments were applied to large-cross-section red pine round timber to control the direction of moisture movement during drying. The drying speed was evaluated through real-time monitoring and factors affecting the occurrence of drying defects were examined.

The initial drying phase was characterized by a rapid decrease in the shell MC, generating significant drying stress owing to the steep MC gradient. Surface treatment was found to be a key factor influencing both the drying

rate and onset of surface checking.

Specifically, the LC treatment effectively alleviated the occurrence of drying checks but resulted in a slower overall drying rate, and it has certain limitations for industrial applications. Conversely, the ES treatment was associated with surface mold growth, suggesting that sealing may have restricted air circulation.

These findings suggest that for large-diameter coniferous species, such as red pine, LC is the optimal strategy for mitigating surface check occurrence. However, considering the practical challenges of industrial applications, future research should focus on optimizing the scale and methods for LC applications. A prudent selection of surface treatment is essential for optimal moisture management and quality enhancement during the air drying of large timber.

CONFLICT of INTEREST

No potential conflict of interest relevant to this article was reported.

ACKNOWLEDGMENT

This research was supported by the Cultural Heritage Smart Preservation and Utilization R&D Program of the Cultural Heritage Administration, National Research Institute of Cultural Heritage (Project No. RS-2021-NC100101).

REFERENCES

Avramidis, S., Lazarescu, C., Rahimi, S. 2023. Basics of Wood Drying. In: Handbook of Wood Science and Technology, Ed. by Niemz, P., Teischinger, A., and Sandberg, D. Springer, Berlin, Germany. pp. 679-706.

Batjargal, B.U., Lee, T., Cho, M., Lee, C.J., Yeo, H. 2023. Effects of pretreatment for controlling internal water transport direction on moisture content profile and drying defects in large-cross-section red pine round timber during Kiln drying. Journal of the Korean Wood Science and Technology 51(6): 493-508.

Batjargal, B.U., Lee, T., Lee, C.J., Oh, J.K., Yeo, H. 2025. Control of internal moisture transfer direction and lateral moisturization to mitigate drying defects in large-cross-section timber. BioResources 20(2): 4761-4775.

Bond, B.H., Espinoza, O. 2016. A decade of improved lumber drying technology. Current Forestry Reports 2(2): 106-118.

Dietsch, P., Franke, S., Franke, B., Gamper, A., Winter, S. 2015. Methods to determine wood moisture content and their applicability in monitoring concepts. Journal of Civil Structural Health Monitoring 5(2): 115-127.

Elustondo, D., Matan, N., Langrish, T., Pang, S. 2023. Advances in wood drying research and development. Drying Technology 41(6): 890-914.

Erber, G., Holzleitner, F., Kastner, M., Stampfer, K. 2017. Impact of different time interval bases on the accuracy of meteorological data based drying models for oak (*Quercus* L.) logs stored in piles for energy purposes. Croatian Journal of Forest Engineering 38(1): 1-9.

Fu, Z., Chen, J., Zhang, Y., Xie, F., Lu, Y. 2023. Review on wood deformation and cracking during moisture loss. Polymers 15(15): 3295.

Fu, Z., Zhao, J., Huan, S., Sun, X., Cai, Y. 2015. The variation of tangential rheological properties caused by shrinkage anisotropy and moisture content gradient in white birch disks. Holzforschung 69(5): 573-579.

Han, Y., Chang, Y.S., Eom, C.D., Lee, S.M. 2019a. Moisture content change of Korean red pine logs during air drying: II. Prediction of moisture content change of Korean red pine logs under different air

drying conditions. Journal of the Korean Wood Science and Technology 47(6): 732-750.

Han, Y., Eom, C.D., Lee, S.M., Park, Y. 2019b. Moisture content change of Korean red pine logs during air drying: I. Effective air drying days in major regions in Korea. Journal of the Korean Wood Science and Technology 47(6): 721-731.

Jiang, Z., Yamamoto, H., Matsuo-Ueda, M., Yoshida, M., Dohi, M., Tanaka, K., Konishi, H. 2023. Effect of high temperature drying with load on reduction of residual stress and correction of warp of Japanese cedar lumber. Drying Technology 41(1): 3-16.

Kang, C.W., Muszyński, L., Hong, S.H., Kang, H.Y. 2016. Preliminary tests for the application of an optical measurement system for the development of a Kiln-drying schedule. Drying Technology 34(4): 483-490.

Kang, H.Y., Muszynski, L., Milota, M.R., Kang, C.W., Matsumura, J. 2011. Preliminary tests for optically measuring drying strains and check formation in wood. Journal of the Faculty of Agriculture, Kyushu University 56(2): 313-316.

Kim, J.H., Yang, S.M., Lee, H.J., Park, K.H., Kang, S.G. 2020. A study on the evaluation and improvement of permeability in radial and tangential section of domestic softwoods. Journal of the Korean Wood Science and Technology 48(6): 832-846.

Kim, K.J., Kim, Y.J., Park, S.Y. 2023. Improvement of physical and drying properties of large diameter and long axis Moso bamboo (*Phyllostachys pubescens*) poles using heat treatment. Journal of the Korean Wood Science and Technology 51(6): 447-457.

Kollmann, F.F.P., Côté, W.A.Jr. 1968. Principles of Wood Science and Technology. I: Solid Wood. Springer-Germany, Berlin.

Lazarescu, C., Watanabe, K., Avramidis, S. 2010. Density and moisture profile evolution during timber drying by CT scanning measurements. Drying Technology 28(4): 460-467.

Lee, C.J. 2020. Effect of kerfing and incising pretreatments on high-temperature drying characteristics of cedar and larch boxed-heart timbers with less than 150 mm in cross section size. Journal of the Korean Wood Science and Technology 48(3): 345-363.

Lee, H.W., Kim, H.O., Lee, D.H., Choi, D.H., Kim, S.G. 2024. Fixed bed drying of sugarcane bagasse using solar energy. Journal of the Korean Wood Science and Technology 52(1): 47-57.

Lee, I.H., Kim, K., Shim, K. 2022. Evaluation of bearing strength of self-tapping screws according to the grain direction of domestic *Pinus densiflora*. Journal of the Korean Wood Science and Technology 50(1): 1-11.

Mori, T., Ariki, A., Enatsu, Y., Sadakane, Y., Tanaka, K. 2025. Study on measurement methods for moisture content inside wood. Buildings 15(15): 2719.

Möttönen, V. 2006. Variation in drying behavior and final moisture content of wood during conventional low temperature drying and vacuum drying of *Betula pendula* timber. Drying Technology 24(11): 1405-1413.

National Heritage Administration. 2024. 2024 Standard Specifications for National Heritage Repair. National Heritage Administration, Daejeon, Korea.

Ogueke, N.V., Nwaizu, P.C., Nwufo, O., Nwaigwe, K., Anyanwu, E.E. 2015. Biomass powered natural convection Kiln for timber drying. Research Journal of Applied Sciences, Engineering and Technology 9(4): 282-287.

Park, Y., Chung, H., Kim, H., Yeo, H. 2020. Applicability of continuous process using saturated and superheated steam for boxed heart square timber drying. Journal of the Korean Wood Science and Technology 48(2): 121-135.

Park, Y., Kim, C., Jeong, H., Lee, H.M., Kim, K.M., Lee, I.H., Kim, M.J., Kwon, G.B., Yoon, N., Lee, N. 2024. Evaluation of the basic properties for the Korean major domestic wood species: I. Korean

red pine (*Pinus densiflora*) in Pyeongchang-gun, Gangwon-do. Journal of the Korean Wood Science and Technology 52(1): 87-100.

Ra, J.B. 2014. Determination of equilibrium moisture content of outdoor woods by using Hailwood-Horrobin equation in Korea. Journal of the Korean Wood Science and Technology 42(6): 653-658.

Routa, J., Kolström, M., Ruotsalainen, J., Sikanen, L. 2015. Precision measurement of forest harvesting residue moisture change and dry matter losses by constant weight monitoring. International Journal of Forest Engineering 26(1): 71-83.

Schmidt, E., Riggio, M. 2019. Monitoring moisture performance of cross-laminated timber building elements during construction. Buildings 9(6): 144.

Sehlstedt-Persson, M., Wamming, T. 2010. Wood drying process: Impact on scots pine lumber durability. Journal of Wood Science 56(1): 25-32.

Shin, J.S., Lee, Y.S., Kim, E.S., Jang, K., Lee, J.S., Seo, J.W. 2025. The effects of climate on the death and growth decline of *Pinus densiflora* Siebold & Zucc. using the annual ring-width time series. Journal of the Korean Wood Science and Technology 53(4): 441-453.

Simpson, W.T. 1973. Predicting equilibrium moisture content of wood by mathematical models. Wood and Fiber 5(1): 41-49.

Simpson, W.T. 1991. Dry Kiln Operator's Manual. Agriculture Handbook. United States Department of Agriculture, Washington, DC, USA.

Srisuchart, K., Tomad, J., Leelatanon, S., Jantawee, S., Matan, N. 2023. Internal stress development within wood during drying: A master curve concept and its application on drying stress evaluation. Drying Technology 41(15): 2516-2532.

Thybring, E.E., Fredriksson, M. 2021. Wood modification as a tool to understand moisture in wood. Forests 12(3): 372.

Ugwu, S.N., Uduji, Z., Nwoke, O.A., Echiegu, E.A., Ugwuishiwu, B.O. 2021. Engineering properties of wood under different drying methods. Global Journal of Engineering and Technology Advances 07(03): 118-124.

Zinad, O.S., Csilla, C. 2024. Review on water vapor diffusion through wood adhesive layer. Journal of the Korean Wood Science and Technology 52(4): 301-318.